THE GEOTHERMAL GRADIENT OF IO: CONSEQUENCES FOR LITHOSPHERE STRUCTURE AND VOLCANIC ERUPTIVE ACTIVITY.
G. Leone[1], L. Wilson[1] and A. G. Davies[2], [1]Lancaster Environment Centre, Lancaster University, Lancaster LA1 4YQ, UK (leone@unix.lancs.ac.uk; l.wilson@lancaster.ac.uk), [2]Jet Propulsion Laboratory, 4800 Oak Grove Drive, Pasadena CA 91109-8099, USA (Ashley.Davies@jpl.nasa.gov)

Introduction: Near-surface sulphur compounds on Io are mobilized by interaction with erupted volcanic materials [1-3], incorporated into eruption products and buried by later eruptions. Thus the internal temperature structure of Io [4] exerts a vital control on the distribution of the recycled volatiles and how they interact with rising magmas. This influences both surface eruption styles [5] and the presence or absence of subsurface magma reservoirs [6].

Methods: To improve estimates of the variation of temperature T with depth z in Io's lithosphere we utilized the basic equations defined by [4]:

$$F_a = V \rho_m [\Delta H + C_{pa} (T_m - T_s)]$$

and

$$\kappa \frac{\partial^2 T}{\partial z^2} = V \frac{\partial T}{\partial z} - \frac{A}{\rho_l c_p}$$

where F_a is the volcanically advected volcanic heat flux per unit area of the planet, V is the resurfacing (i.e. surface burial) rate, ρ_m is the density of erupted magma (2700 kg m^{-3}), ρ_l is the depth-dependent bulk density of the lithosphere, C_p and κ are the magma specific heat and thermal diffusivity, respectively, ΔH is the latent heat of magma crystallization (4.5×10^5 J kg^{-1}), A is the radiogenic heat production rate in the lithosphere (initially assumed equal to the bulk Earth value $\sim 2.4 \times 10^{-8}$ W m^{-3}, though varying the value by a factor of 2 has a negligible influence on the results), and T_m and T_s are the magma temperature in the mantle source region and the mean surface temperature, 1500 K and 100 K, respectively. Average values of the thermal parameters C_p and κ were used by [4] to make an analytical solution of these equations possible, but we have used a numerical solution method implemented as a FORTRAN program allowing us to make C_p and κ continuous functions of temperature based on data from [7] and [8]. Over the 100 to 1500 K temperature range C_{pa} is found to be equal to 1040 J kg^{-1} K^{-1}. We evaluate the bulk density of the lithosphere rocks by assuming a surface porosity void space fraction v_{v0}, up to 0.3 (i.e. 30% porosity) and integrating numerically the increase of density ρ_l and pressure P as the void space compacts like

$$v_v = v_{v0} \exp(-\lambda P)$$

where $\lambda = 1.18 \times 10^{-8}$ Pa^{-1} is a constant independent of the acceleraton due to gravity [9] and

$$\rho_l = \rho_c (1 - v_v)$$

where ρ_c is the density of an assumed mixture of silicates with density 3000 kg m^{-3} at the surface and bulk modulus ~10 GPa, and SO_2 and S in the mass ratio of 5:1, both with density ~2000 kg m^{-3}. The ratio of silicates to volatiles is a variable in the model. We include the variation of acceleration due to gravity with depth:

$$g = g_0 [(R - z)/R]$$

where R is the radius of Io, ~1815 km, and g_0 is the acceleration due to gravity at the surface, ~1.8 m s^{-2}. Finally we correct the thermal diffusivity, defined as $\kappa = k / (\rho_l C_p)$, for the dependence of thermal conductivity k on porosity:

$$k / k_0 = 1 - 1.738 v_v + 0.8228 v_v^2$$

where k_0 is the value of k when $v_v = 0$.

Results: The key model variable is the volcanic heat flux, F_a, for which we assume a present-day value of 2.4 W m^{-2} [10-13]. We then explore the consequences of using smaller values to reflect the possibly complex spatial and temporal history of Io's heat flux [14-18].

Table 1 shows how thermal parameters vary with depth for the present-day heat flow F_a and a lithosphere thickness of 30 km. Temperature initially increases slowly with depth and then rises very rapidly to the mantle temperature. Figure 1 shows how varying F_a changes the temperature structure. Our results broadly agree with those of [4]: our model produces somewhat higher temperatures at intermediate depths in the lithosphere with a corresponding less-rapid increase near the lithosphere base.

Consequences for volcanism: For the current heat flow, each temperature profile in Figure 1 gives the depths (~21 and 26 km), temperatures (209 and 421 K) and pressures (92 and 118 MPa) at which SO_2 and sulphur melt. We find the bulk density of rising magma as it incorporates various amounts of these volatiles from aquifers produced by melting and compare this with the lithosphere density through which the magma rises:

(a) volatile-free magmas are positively buoyant at the base of the lithosphere for surface void space fractions, v_{v0}, < ~0.38 but become neutrally buoyant at some depth, where they may form intrusions growing into magma reservoirs. The neutral buoyancy depths for v_{v0} = 0.1, 0.2 and 0.3 are 0.2, 14.8 and 23.0 km, respectively. Only if $v_{v0} = 0$ will a volatile-free magma be positively buoyant all the way to the surface.

(b) magmas absorbing more than ~5 mass % of the S_2-SO_2 mixture from deep aquifers will be positively buoyant at all depths for all plausible values of v_{v0}.

(c) magmas absorbing 10-30 mass % of volatiles, the range implied by the highest eruption plumes, will be very positively buoyant, and the pressure gradients driving their eruptions will be large, suggesting that there should be a positive correlation between mass eruption rate and volatile content.

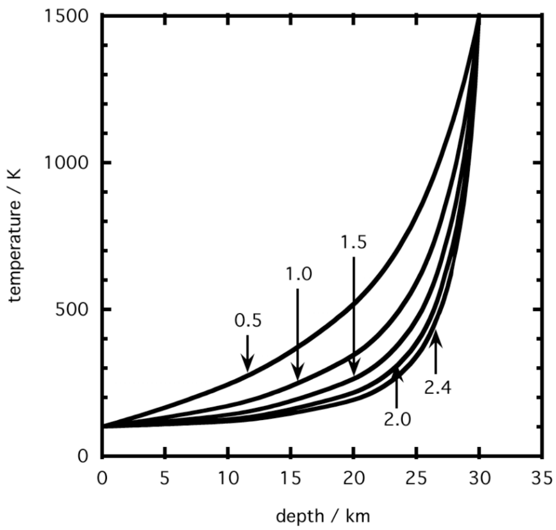

Figure 1. Variation of temperature T with depth z for 5 values of the advected volcanic heat flux F_a.

References: [1] Kieffer, S.W. (1982) pp. 647-723 in *Satellites of Jupiter*, Univ. Ariz. Press. [2] Kieffer, S.W., Lopes-Gautier, R., McEwen, A., Smythe, W., Keszthelyi, L. & Carlson, R. (2000) Science 288, 1204. [3] Milazzo, M.P., Keszthelyi, L.P., McEwen, A.S. (2001) JGR 106, 33,121. [4] O'Reilly, T.C. & Davies, G.F. (1981) GRL 8, 313. [5] Cataldo, E., Wilson, L., Lane, S. & Gilbert, J. (2002) JGR 107 (E11), 5109. [6] Leone, G. & Wilson, L. (2001) JGR 106, 32983. [7] Whittington, A.G., Hofmeister, A.M. & Nabelek, P.I. (2009) Nature 458, 319 and Nature, 459, 122. [8] Robie, R.A., Hemingway, B. S. & Wilson, W.H. (1970) Proc. Apollo 11 Lunar Sci. Conf., 2361. [9] Head, J.W. & Wilson, L. (1992) JGR 97, 3877. [10] Spencer, J. R. et al. (2000) Science, 288, 1198. [11] Rathbun, J.A. et al. (2004) Icarus, 169, 127. [12] Veeder, G.J., Matson, D.L. Johnson, T.V., Davies, A.G. & Blaney, D.L. (2004) Icarus, 169, 264. [13] Lainey, V., Arlot, J.-E., Karatekin, Ö. & Van Hoolst, T. (2009) Nature 459, 957. [14] Ojakangas, G.W. & Stevenson, D.J. (1986) Icarus 66, 341. [15] Segatz, M., Spohn, T., Ross, M.N. & Schubert, G. (1988) Icarus 75, 187. [16] Tackley, P.J., Schubert, G., Glatzmaier, G.A., Schenk, P., Ratcliff, J.T. & Matas, J.P. (2001) Icarus 149, 79. [17] Hussmann, H. & Spohn, T. (2004) Icarus 171, 391. [18] Lainey, V. & Tobie, G. (2005) Icarus 179, 485.

Table 1. Variation with depth, z, below the surface of Io of the bulk density of the lithosphere, ρ_l, the lithostatic pressure, P, the temperature, T, and the implied thermal conductivity, k, specific heat, C_p, and thermal diffusivity, κ, of the lithospheric rocks. Model parameters are advective (volcanic) heat flux F_a = 2.4 W m^{-2}, radiogenic heat production rate $A = 2.4 \times 10^{-8}$ W m^{-3}, lithosphere thickness 30 km, surface void space fraction v_{v0} = 0.3, surface temperature T_0 = 100 K and magma temperature T_m = 1500 K.

z / km	ρ_l / (kg m^{-3})	P / MPa	T / K	k / (W m^{-1} K^{-1})	C_p / (J kg^{-1} K^{-1})	κ / (m^2 s^{-1})
0.0	2096	0.0	100	1.47	226	3.10×10^{-6}
10.0	2440	40.9	117	2.36	286	3.37×10^{-6}
20.0	2672	86.7	189	3.29	510	2.41×10^{-6}
25.0	2752	110.8	326	3.24	815	1.45×10^{-6}
26.0	2766	115.7	386	3.04	898	1.23×10^{-6}
27.0	2779	120.6	474	2.72	982	9.97×10^{-7}
28.0	2791	125.5	615	2.29	1078	7.61×10^{-7}
29.0	2802	130.5	882	1.78	1162	5.47×10^{-7}
29.5	2808	133.0	1122	1.75	1197	5.19×10^{-7}
29.6	2809	133.5	1185	1.74	1207	5.12×10^{-7}
29.7	2810	134.0	1252	1.72	1216	5.04×10^{-7}
29.8	2811	134.5	1327	1.71	1227	4.96×10^{-7}
29.9	2812	135.0	1410	1.69	1239	4.86×10^{-7}
30.0	2813	135.5	1500	1.67	1252	4.75×10^{-7}